PAPER

Check for updates

Nitrogen-doped graphene and titanium carbide nanosheet synergistically reinforced epoxy composites as high-performance microwave absorbers

Yuchang Qing, [iD] * Hanyi Nan, Fa Luo and Wancheng Zhou

The electromagnetic (EM) properties of both nitrogen-doped graphene (N-GP) and Ti_3C_2 nanosheets as hybrid absorbers were investigated in the frequency range of 2–18 GHz. The values and frequency dependencies of EM properties of such hybrid absorbers can be adjusted by the combination of the unique microstructure and dielectric characteristics of the N-GP and Ti_3C_2 nanosheets. The minimum reflection loss (RL) reaches up to −52 dB and the bandwidth below −10 dB can be obtained in the frequency range of 10.9–18 GHz with a sample thickness of 1.4 mm. These results suggest that N-GP and Ti_3C_2 nanosheets as hybrid absorbers are highly promising fillers for dielectric and EM applications, especially for thin-thickness, broadband absorption microwave absorbers.

1. Introduction

The unique properties of 2D nanosheets, which are lightweight, flexible and have high mechanical strength, high thermal conductivity, high specific surface area and excellent electronic properties, have enabled rapid development in their fundamental research and practical applications. They can be used in electronics, optoelectronics, catalysis, energy storage devices and so on.[1–7] More recently, 2D nanosheets with outstanding dielectric properties have received significant investigation in the field of electromagnetic (EM) and microwave absorption due to their corresponding dimensional structures, high specific surface area and clustered defects.[8–16] Ultrathin graphene (GP) and graphene nanosheets (GNs), with low density, high aspect ratio and high conductivity, exhibit good microwave absorption and indicate the GP and GNs could be very promising microwave absorber. The dielectric properties and microwave absorption performance of few-layered MoS_2 nanosheets were reported, and the minimum reflection loss (RL) value of MoS_2 nanosheets/wax with 60 wt% loaded is −38.42 dB at a thickness of 2.4 mm.[15] A thin sample consisting of 10 wt% MoS_2/RGO hybrid in the wax matrix exhibited an effective microwave absorption bandwidth of 5.72 GHz at the thickness less than 2.0 mm.[16]

The MXenes with 2D early transition metal carbides and carbonitrides are produced by selective etching of the A element from the MAX phases. MXenes combine the metallic conductivity of transition metal carbides with unique morphologies render them strong candidates for many applications.[5–7] Up to now, few experimental results that exist to date have explored the EM properties of MXenes, which have a wide range of potential applications, such as EM interference shielding, actuators, microwave absorber, capacitors, and photovoltaic. More recently, the RL values of the Ti_3C_2 nanosheets filled composites exceeding −11 dB (more than 92% absorption) in the frequency range of 12.4–18 GHz with a thickness of 1.4 mm, suggests that Ti_3C_2 nanosheets with unique dielectric properties are highly promising fillers for dielectric and EM applications.[17]

However, single GP or GNs filled composites could not meet the demands of ideal microwave absorbing materials (MAMs) because the intrinsic high permittivity and low permeability of such materials, lead to poor impedance matching and further affect absorbing properties. The effectiveness of a MAM is mainly depended on its EM characteristics, which means the key point to obtain thin-layer broadband GP-filled MAMs is controlling the EM properties of such composites. In order to effectively improve microwave absorptions, attentions have been directed toward adding magnetic and/or dielectric fillers into a matrix, for instance, adding magnetic materials to GP-filled composites to enhance their complex permeability, to satisfy the demand of low reflection over a broad frequency range.[14] Hybrid absorbers possess the advantages of its individual components and may exhibit new EM properties and functions for practical applications. The components of hybrid absorbers can be chosen from a wide range of materials with versatile morphologie.[18] Nevertheless, to our best knowledge, investigations on the EM properties and microwave absorption

State Key Laboratory of Solidification Processing, School of Materials Science and Engineering, Northwestern Polytechnical University, Xi'an 710072, China. E-mail: qtvbgyta@163.com; qingyuchang@nwpu.edu.cn; Fax: +86 29 8849 4574

performance of nitrogen-doped graphene (N-GP)/Ti_3C_2 nanosheets as hybrids absorbers have yet to report to date.

The dielectric properties and microwave absorption of N-GP and Ti_3C_2 nanosheets filled epoxy composites were investigated in the frequency range of 2–18 GHz. Attributed to unique microstructure and suitable EM properties of N-GP and Ti_3C_2 nanosheets, N-GP and Ti_3C_2 nanosheets as hybrid absorbers filled composites have significant development potential to obtain suitable values and frequency dependency of EM properties. The minimum RL value reaches up to −52 dB and the bandwidth below −10 dB can be obtained in the frequency range of 10.9–18 GHz with a thickness of 1.4 mm, indicates that such hybrid absorbers can be good candidates for fabricating microwave absorbers with thin-thickness, wide bandwidth and enhanced microwave absorption.

2. Materials and methods

The N-GP was prepared *via* a CVD process by using a 20 nm thick of Cu film on a Si substrate as the catalyst, and NH_3 and CH_4 (NH_3/CH_4 ratios of 1 : 1.5) as the N source and C source, respectively.[19] After growth, the sample was cooled to room temperature under H_2 and Ar ambient. The Ti_3C_2 nanosheets were produced by selective etching of the Al element from Ti_3AlC_2 powders. In a typical process, the Ti_3AlC_2 powders were immersed in 50% HF for 3 h at room temperature. The resulting suspension was then washed several times using deionized water and centrifuged to separate the powders. The Ti_3AlC_2 powders after HF treatment were added into the ethyl alcohol and then ultrasonic treatment for 1 h to obtain the Ti_3C_2 nanosheets. The matrix used in this work is epoxy resin and the cure agent is polyamide resin, which were supplied by XI AN Leeo Technological Co.

In order to determine the characteristic of the composite, four samples containing different contents of N-GP and/or Ti_3C_2 nanosheets were manufactured and tested. The sample ID was specified by the content of filler. Sample G2, G2T20, G2T30 and T40 indicate a composition consisting of 2 wt% N-GP, 2 wt% N-GP and 20 wt% Ti_3C_2 nanosheets, 2 wt% N-GP and 30 wt% Ti_3C_2 nanosheets, and 40 wt% Ti_3C_2 nanosheets, respectively. Epoxy resin and polyamide resin were mixed in 4 : 1 weight ratio for preparing matrix used in the experiment.

In order to fully achieve the reinforced potential of N-GP and Ti_3C_2 nanosheets, a highly homogenized dispersion of the fillers is required. First, the N-GP and/or Ti_3C_2 nanosheets were dispersed in acetone using an ultrasonic bath, at room temperature, for 4 h. Then the previously prepared matrix was proportionally weighed and added, followed by stirring at 2000 rpm for 10 min to have the uniform distribution of N-GP and/or Ti_3C_2 nanosheets. In order to reduce the voids, which could detrimentally affect the properties of the final sample, the bubbles should be avoided with the solvent properly evaporated by following steps: the mixture of the resin and absorbers pre-heated to 60 °C in a vacuum drying oven to reduce its viscosity, then evaporated acetone and eliminated the entrapped air, which also can avoid the re-aggregation of N-GP and Ti_3C_2

nanosheets. Finally, the samples were cured at 120 °C for 4 h to obtain well-shaped hard discs.

The morphology of the samples was observed by field emission scanning electron microscopy (FE-SEM) (Model JSM-6360, JEOL, Tokyo, Japan) and transmission electron microscopy (TEM) (Model JEM-2100, JEOL, Tokyo, Japan). Raman spectra were recorded on a Renishaw RM 1000 confocal system spectrometer. X-ray photoelectron spectroscopy (XPS) measurements were examined by an XPS spectrometer (ESCA-LAB250, Thermo, USA). Cylindrical toroidal specimen (out diameter of 7.0 mm and inner diameter of 3.03 mm) were prepared for EM properties measurement in the frequency range of 2–18 GHz, using the T/R coaxial line method by a network analyzer (Agilent Technologies E8362B: 10 MHz to 20 GHz).

3. Results and discussions

TEM images (Fig. 1a) show the N-GP has a flexible and rumpling morphology, which indicates the N-GP is flexible, and such rumpling comes from the growth process and the cooling process.[19] The exfoliated Ti_3C_2 nanosheets with typical of
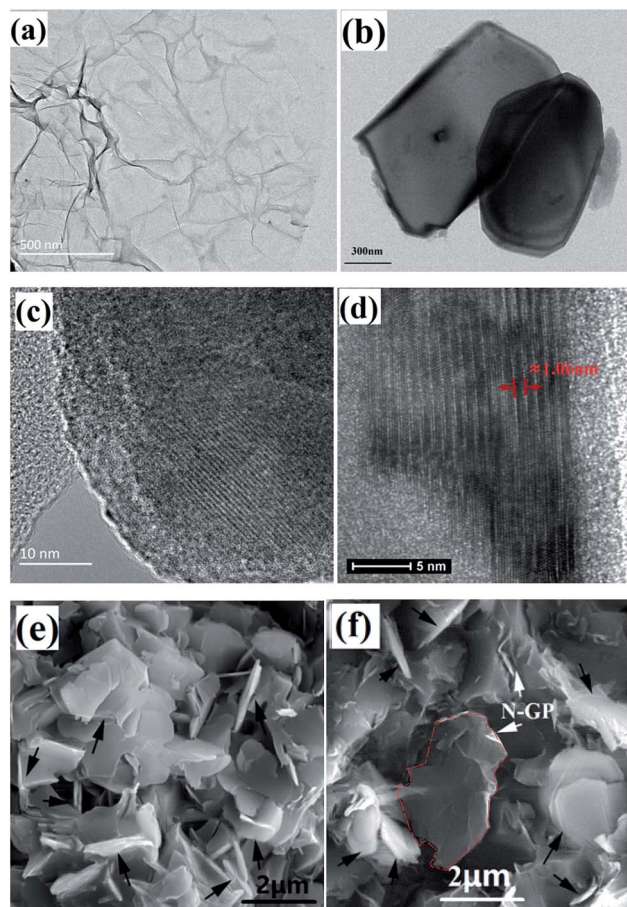

Fig. 1 TEM image of (a) the N-GP and (b–d) TEM image of the exfoliated Ti_3C_2 nanosheets. Typical SEM images of the N-GP and/or Ti_3C_2 nanosheets filled composites, (e) sample T40 and (f) sample G2T30 (the black arrows for the Ti_3C_2 nanosheets).

MXenes structure were obtained, which clearly confirms the successful exfoliation of individual Ti_3AlC_2 particles, as shown in Fig. 1b and c. The HRTEM image reveals the detailed crystalline structure of the Ti_3C_2 nanosheets, and the multilayer stacks are comprised of about 16 layers, and the corresponding layer spacing in the *c*-direction is ~10.6 Å (Fig. 1d).

The Ti_3C_2 nanosheets, acting as a three-phase particle, are also thought to improve the dispersion of N-GP in the final composite, which can lead to a dramatic improvement of N-GP and Ti_3C_2 nanosheets dispersion throughout the matrix. Fig. 1e and f show the dispersions of N-GP and/or Ti_3C_2 nanosheets, indicating that the use of ultrasonic treatment and intensely mechanical stirring is an effective way to enhance the dispersion N-GP and Ti_3C_2 nanosheets throughout the matrix.

Typical D band (from defect and amorphous carbon) and G band (from graphite) are detected at ~1352 and ~1578 cm^{-1} for the N-GP, as shown in Fig. 2. The ratio between the intensities of the D and G bands (I_D/I_G) is, about 0.94 for N-GP, considered to be the ratio of structural defects and domain size in graphitic materials. There are many factors, which can affect the position of the G band, such as doping, layer numbers, defects, strains, substrate, *etc.*[20] The shift of the G band and high value of I_D/I_G for the N-GP indicates N doping break the sp^2 carbon domains in the 2D hexagonal structure to form sp^3 defect and introduce large amount of topological defects. The observation of N doping causes a downshift of the G band is also similar to those reported N-doped CNTs and N-GP.[19] Raman spectra of Ti_3C_2 after HF treatment are also shown in Fig. 2. Compared with Ti_3AlC_2,[6] peaks assigned to Al–Ti vibrations vanished after treatment, while peaks involve only Ti–C vibrations merged, broadened, downshifted, and the peak intensities are also
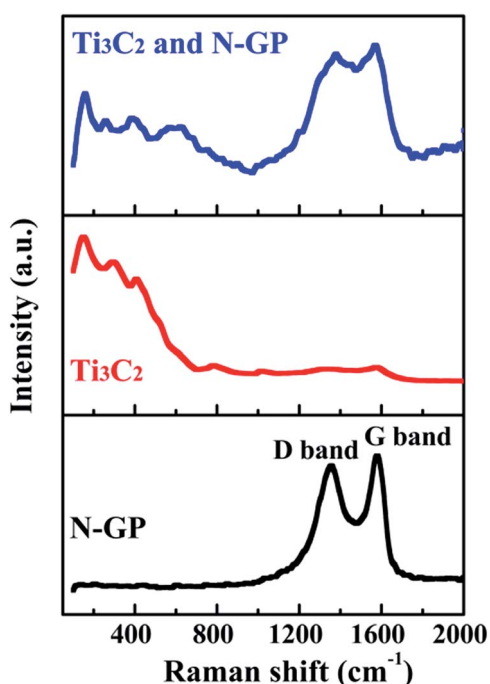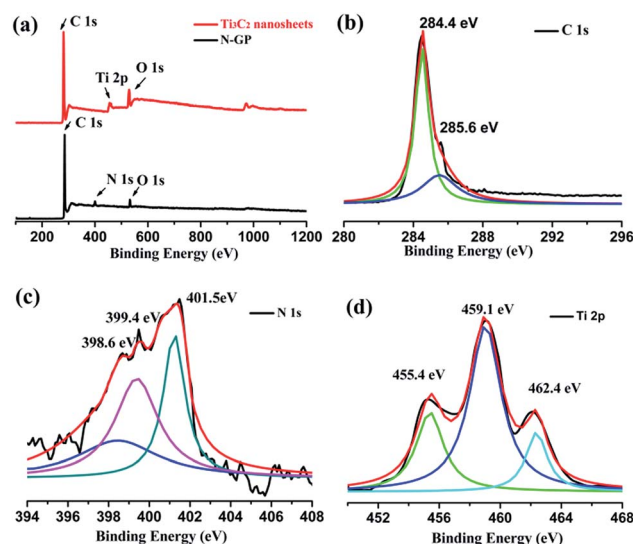

Fig. 3 (a) XPS spectra of the G-NP and Ti_3C_2 nanosheets. (b) High-resolution XPS C 1s spectrum and (c) XPS N 1s spectrum of the G-NP. (d) High-resolution Ti 2p spectra of Ti_3C_2 nanosheets.

much reduced. Such changes observed in Raman spectra of Ti_3C_2 after HF treatment confirms the loss of Al from the structure, and are in agreement with the previously reported Raman spectra of the Ti_3C_2 nanosheets prepared from Ti_3AlC_2 powders with HF treatment.[5–7]

The XPS spectra of G-NP confirm the N doping of the graphene, the peaks at 284.4, 401.5, and 532.4 eV correspond to C 1s of sp^2 C, N 1s of the doped N, and O 1s of the absorbed oxygen, respectively, and the atomic percentage of N in the sample is about 5.6 at%. Oxygen can be included due to exposure to the air. No extra peaks except C, N and O were observed, indicating the high purity of the product. The main peak at 284.4 eV corresponds to the graphite-like sp^2 C, indicating most of the C atoms in the N-doped graphene are arranged in a conjugated honeycomb lattice. The small peaks at 285.6 eV reflect different bonding structure of the C–N bonds, such as the N-sp^2 C bonds, and would originate from substitution of the N atoms, defects or the edge of the graphene sheets.[20] The high resolution XPS spectrum of N 1s (Fig. 3c) can be resolved into three bonds, which locate at 398.6, 399.4 and 401.5 eV, respectively. The main peak at 401.5 eV is associated to the graphitic N bonding, which refers to the N atoms replacing the C atoms inside of the graphene layers, and is in good agreement with the spectral feature of reported CVD N-GP.[19] The small peaks at 398.6 and 399.4 eV correspond to pyridinic N and pyrrolic N, respectively. They refer to the N atoms which are located in a π conjugated system and contribute to the π system with one or two p-electrons, respectively. The Ti 2p XPS results of Ti_3C_2 nanosheets exhibit the four predominant peaks at ~455.4, 459.1, and 462.4 eV, which correspond to the Ti–O (2p^1), Ti–O (2p^3), and Ti–C (2p^3), respectively, as shown in Fig. 3d. The presence of Ti–C and Ti–O bonds was evident from both spectra, indicating the formation of Ti_3C_2 MXenes after treatment. The O 1s main signal (at ≈530.1 cm^{-1}) suggest the

Fig. 2 Raman spectra of the N-GP, Ti_3C_2 nanosheets, and the N-GP/ Ti_3C_2 nanosheets.

presence of an OH group.[21] As mentioned above, defects and functional groups existed for both of N-GP and Ti_3C_2 nanosheets, which can induce dielectric polarization relaxation and group's electronic dipole polarization relaxation, which is believed to be favorable for microwave absorption performance.

Interactions between the microwave-absorber filled composites and EM waves in the microwave frequency band can be expressed by relative complex permittivity ($\varepsilon^* = \varepsilon' - j\varepsilon''$) and complex permeability ($\mu^* = \mu' - j\mu''$). For the relative complex permittivity of the absorber, the real part of the relative complex permittivity (ε') is proportional to the quantity of the electric charges stored on the surface when the composite is under an applied electric field. The imaginary part of the relative complex permittivity (ε'') accounts for the energy loss *via* dissipative mechanisms of the composites.[22–28] Fig. 4 shows the frequency dependencies of the ε' and ε'' of the epoxy composites filled with N-GP and/or Ti_3C_2 nanosheets as absorber. Both the values of ε' and ε'' of the 2 wt% N-GP and 30 wt% Ti_3C_2 nanosheets-filled composites in the measured frequency range, about 39.2–11.7 and 9.5–4.5, respectively, are much higher than those of 40 wt% Ti_3C_2 nanosheets-filled composites, about 18.0–9.1 and 6.2–3.6, respectively. The value of ε' is an expression of the polarization of a material (consisted of interface and orientation polarization) under the EM field.[29] It is found that using N-GP and Ti_3C_2 nanosheets as hybrid absorber result in a significant enhancement of ε' of such composites. A large quantity of surface electric charges and defects can be created by using the N-GP

and Ti_3C_2 nanosheets as absorbers, which are obtained by an aggressive exfoliation process.[17] The enhanced number of interfaces between N-GP and Ti_3C_2 nanosheets with the epoxy matrix result in more electron relaxation polarization and interfacial polarization, thus, it should be possible to obtain the higher values of ε' for the N-GP and Ti_3C_2 nanosheets filled composites. A large number of microcapacitors between the N-GP and Ti_3C_2 nanosheets were formed due to their unique 2D microstructure, which results in the increasement of the polarization mechanisms and also is responsible for the enhancement of the value of ε'. Moreover, the ε' of the N-GP and Ti_3C_2 nanosheets filled composites (sample G2T30) shows an apparent decrease with increasing frequency than that of the single N-GP or Ti_3C_2 nanosheets filled composites.

The values of ε'' mainly depend on two different factors in the microwave frequency range: relaxation and/or polarization phenomenon and electrical conductivity, which can be expressed by the equation: $\varepsilon = \varepsilon''_{relax} + \sigma/(\omega\varepsilon_0)$, where ε''_{relax} is the relaxation polarization in this case, σ is the electrical conductivity, ε_0 is the dielectric constant in vacuum, and ω is the angular frequency.[30] Thus, the ε'' mainly characterizes the capacity of dielectric loss and is determined by the electrical conductivity and relaxation polarization of such composites. The values of ε'' of the sample G2T20 (2 wt% N-GP and 20 wt% Ti_3C_2 nanosheets filled composites) are slightly higher than that of the sample T40 (40 wt% Ti_3C_2 nanosheets filled composites), as shown in Fig. 4b. Obviously, the high value of ε'' of sample G2T20 is caused by added N-GP, which comes from the low resistivity of N-GP and the formation of the N-GP conducting network. Simultaneously, interfacial polarization and the associated relaxation may be also making great contributions to improvement of ε'' value, due to the combination of N-GP and Ti_3C_2 nanosheets. Additionally, the existence of polar functional groups and defects remaining in the N-GP and Ti_3C_2 nanosheets can also increase the dipolar polarization in the composites, which will contribute to the dielectric loss by presenting a higher ε'' value. The microstructure and polarization of the N-GP and Ti_3C_2 nanosheets affect the formation of the microcapacitors network and the evolution of conductive/dielectric loss, which can influence the values and frequency dependencies of both ε' and ε''.[31–34] Therefore, it is reasonable to consider the enhanced values of ε' and ε'' due to the unique microstructure, larger internal boundary layer capacitance, and defects in such N-GP and Ti_3C_2 nanosheet-filled composites, which are the most significant factors affecting the EM properties and absorption performance of such composites. Results of EM properties show that using both N-GP and Ti_3C_2 nanosheets as absorber can change the values and frequency dependencies of both ε' and ε'' in the measured frequency range. Furthermore, the values of ε' and ε'' of the N-GP and Ti_3C_2 nanosheets filled composite also can be tuned by an adjustment of the nature and content of the filler particles, which offer multiple degrees of freedom to tune overall effective permittivity and play a key role in improving the EM absorption performance.

The main requirements for the EM absorbers are expected to have strong microwave absorption in a wide frequency range,
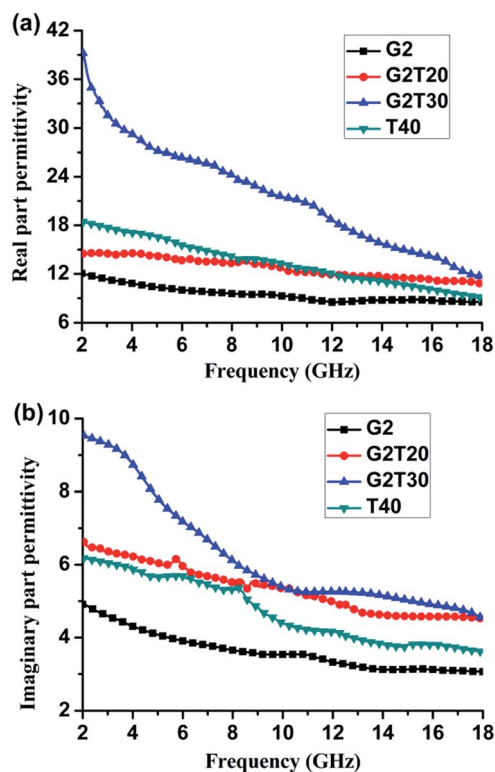

Fig. 4 Frequency dependencies of the (a) real and (b) imaginary part of the relative complex permittivity of the N-GP and Ti_3C_2 nanosheets filled epoxy composites in the frequency range of 2–18 GHz.
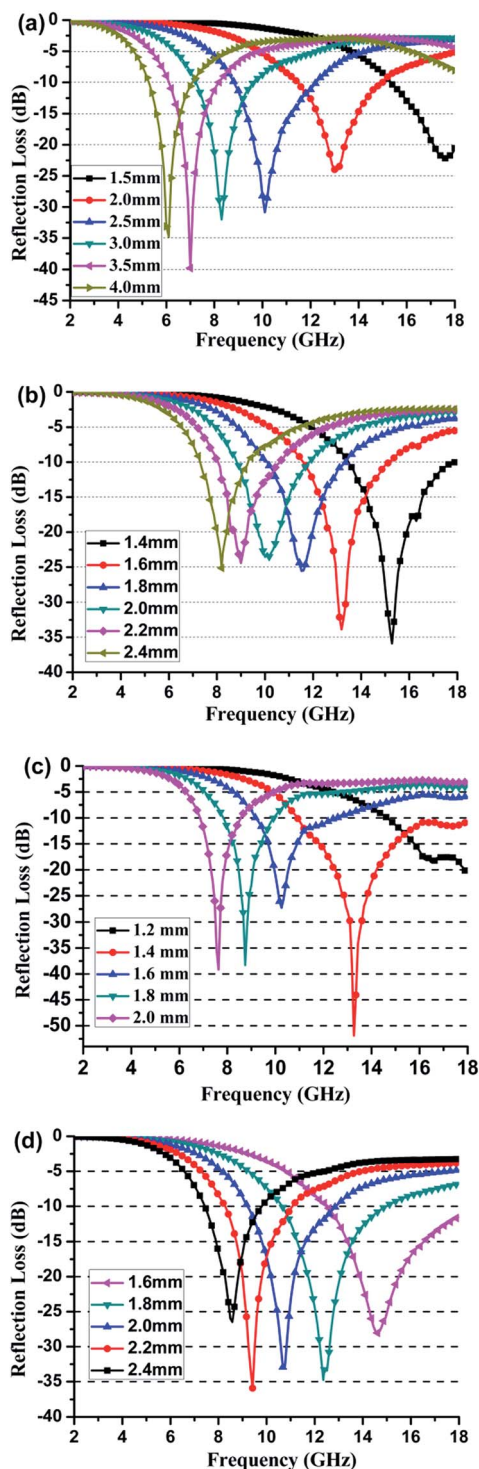
Fig. 5 Frequency dependent of the RL of composite containing different content of N-GP and/or Ti$_3$C$_2$ nanosheets, (a) sample G2, (b) sample G2T20, (c) sample G2T30 and (d) sample T40.

with lightweight and thinner thickness. High RL values of the MAMs over a broad frequency range can be common achieved by the appropriate value and frequency dependence of EM properties.[35–40] Fig. 5 shows the values of RL of the N-GP and/or Ti$_3$C$_2$ nanosheets filled composites in the frequency of 2–18

GHz, which was calculated based on the measured values of ε' and ε'' according to the transmission line theory. The real and imaginary part of relative complex permeability of N-GP and/or Ti$_3$C$_2$ nanosheets is almost 1 and 0 in the whole measured frequency range, due to the weak magnetic characteristics of both N-GP and/or Ti$_3$C$_2$ nanosheets.

Therefore, the values of RL of the N-GP and/or Ti$_3$C$_2$ nanosheets filled composites are mainly depended on the values of ε' and ε'' and dielectric loss. As shown in Fig. 5a, the RL values of the 2 wt% N-GP filled composites can only obtain some high RL value under larger thickness at specific single frequencies, *i.e.* the minimum value of RL is about −31 dB and the absorption bandwidth ≤−10 dB is about 3.3 GHz (range from 8.9 to 12.2 GHz) with a sample thickness of 2.5 mm. Furthermore, the absorption bandwidth of 2 wt% N-GP filled composite is narrow at each single thickness when the composite thickness range from 1.5 to 4 mm. Compared with the RL values of the 2 wt% N-GP filled composites, the 40 wt% Ti$_3$C$_2$ nanosheets filled composites obtain some high RL under thinner thickness, *i.e.*, the minimum RL is about −33 dB and the absorption bandwidth ≤−10 dB is about 3.7 GHz (range from 9.2 to 12.9 GHz) with a sample thickness of 2.0 mm. Compared with the single absorber (N-GP or Ti$_3$C$_2$ nanosheets) filled composites, the composites filled with N-GP and Ti$_3$C$_2$ nanosheets, especially for sample G2T30, had much high RL values, wide absorption bandwidth and thin-thickness, the minimum RL reaches up to −52 dB with the absorption bandwidth ≤−10 dB is about 7.1 GHz (range from 10.9 to 18 GHz) under a thickness of 1.4 mm. A detailed comparison of the minimum RL value and absorption bandwidth of N-GP and/or Ti$_3$C$_2$ nanosheets filled composites and other representative 2D nanosheets filled composites are summarized in the Table 1. It is obviously indicate that N-GP and Ti$_3$C$_2$ nanosheets filled MAMs with high minimum RL value, wider absorption bandwidth and thin-thickness than those reported single layer MAMs.

The absorption frequency ranges and corresponding thicknesses of the MAMs were two key factors for EM applications, and many results show that it is quite a challenge to obtain good absorption performance and thin-thickness at the same time.[41–47]

Interesting, the RL values of sample were enhanced while the corresponding optimal thickness was decreased for the N-GP and Ti$_3$C$_2$ nanosheets filled composites. Firstly, the unique microstructure and extremely high defects of the N-GP and Ti$_3$C$_2$ nanosheets may provide more dielectric polarization induce by the EM wave, which have a significant contribution towards improving both ε' and ε'' under lower absorber content. The improved ε' and ε'' of the N-GP and Ti$_3$C$_2$ nanosheets-filled composites showed in Fig. 4a is generally considered as a significant factor on the dielectric properties and corresponding microwave absorption performances.[44] Secondly, the extreme thinness and high specific surface area of N-GP and Ti$_3$C$_2$ nanosheets could increase the propagation paths for the incident waves inside the samples. The corrugated N-GP and Ti$_3$C$_2$ nanosheets may scattered the EM waves with multiple internal reflection modes are also key point for the

Table 1 Comparison of values of RL of the N–GP and Ti_3C_2 nanosheets filled composites and typical reported 2D nanosheets filled composites in recent literatures

Absorber and content	Thickness (mm)	Minimum RL value (dB)	Bandwidth RL < −10 dB (GHz)	Ref.
2 wt% N-GP + 30 wt% Ti_3C_2 nanosheets	1.4	−52	10.9–18	This work
50 wt% FeCo/GP	2.5	−40.2	7.6–12.1	10
60 wt% MoS_2 nanosheets	2.2	−47.8	11–15.5	11
60 wt% MoS_2 nanosheets	2.4	−38.4	9.6–13.8	15
10 wt% MoS_2/reduced GO	1.9	−26	12.3–18	16
50 wt% Ti_3C_2 nanosheets	1.4	−17	12.4–18	17
50 wt% annealed Ti_3C_2 MXenes	1.85	−45	9.6–12.4	21

enhancement of the values of RL.[45] Moreover, the proper values and frequency dependencies of ε' and ε'' also lead to the reduction of optimal thickness and enhanced absorption of N-GP and Ti_3C_2 nanosheets-filled composites. These results indicate the enhancement of microwave absorption is associated with the suitable values and frequency dependence of dielectric properties, which results from the unique microstructure, content and EM characteristic of the fillers by combining advantages of the N-GP and Ti_3C_2 nanosheets. Thus, the enhanced EM wave absorption properties result from the proper complementarity between the appropriate values and frequency dependencies of the ε' and ε'' of such MAMs.

The values and frequency dependencies of the ε' and ε'' of such N-GP and Ti_3C_2 nanosheets-filled composites can also be further optimized by changing the N-GP and/or Ti_3C_2 nanosheets content. These results indicate that N-GP and Ti_3C_2 nanosheets-filled composites with enhanced microwave absorption and thin-thickness can be obtained simply by optimizing the content, composition and dielectric properties of the absorber. Most importantly, the N-GP and Ti_3C_2 nanosheets-filled composites developed here could act as thin-layer MAMs with wideband and enhanced microwave absorption, and can be simply applied to the industrial scale.

4. Conclusions

N-GP and Ti_3C_2 nanosheets filled composites with high microwave absorption were prepared. The N-GP and Ti_3C_2 nanosheets filled absorbing materials with enhanced values of ε' and ε'' is mainly due to their the unique microstructure and extremely high defects of the N-GP and Ti_3C_2 nanosheets, larger internal boundary layer capacitance, and the formation of the microcapacitors network and the evolution of conductive/dielectric loss. Both the values of ε' and ε'' of the N-GP and Ti_3C_2 nanosheets filled composite can be tuned by an adjustment of the nature and content of the filler particles, which improved the EM absorption performance. The minimum RL of sample G2T30 reaches up to −52 dB with the absorption bandwidth $\leq$−10 dB is about 7.1 GHz (range from 10.9 to 18 GHz) under a thickness of 1.4 mm. Therefore, the N-GP and Ti_3C_2 nanosheets-filled composites developed here could act as thin-layer MAMs with wideband and enhanced microwave absorption.

Notes and references

1 A. K. Geim, *Science*, 2009, **324**, 1530.
2 J. N. Coleman, M. Lotya, A. O'Neill, S. D. Bergin, P. J. King, U. Khan, *et al.*, *Science*, 2011, **331**, 568.
3 S. Z. Butler, S. M. Hollen, L. Cao, Y. Cui, J. A. Gupta, H. R. Gutiérrez, *et al.*, *ACS Nano*, 2013, 7, 2898.
4 V. Nicolosi, M. Chhowalla, M. G. Kanatzidis, M. S. Strano and J. N. Coleman, *Science*, 2013, **340**, 1226419.
5 M. Naguib, O. Mashtalir, J. Carle, V. Presser, J. Lu, L. Hultman, *et al.*, *ACS Nano*, 2012, **6**, 1322.
6 M. Naguib, M. Kurtoglu, V. Presser, J. Lu, J. Niu, M. Heon, *et al.*, *Adv. Mater.*, 2011, **23**, 4248.
7 M. Naguib, V. N. Mochalin, M. W. Barsoum and Y. Gogotsi, *Adv. Mater.*, 2013, **26**, 992.
8 Y. C. Qing, Q. L. Wen, F. Luo and W. C. Zhou, *J. Mater. Chem. C*, 2016, **4**, 4853.
9 Y. C. Qing, Q. L. Wen, F. Luo, W. C. Zhou and D. M. Zhu, *J. Mater. Chem. C*, 2016, **4**, 371.
10 X. Li, J. Feng, Y. Du, J. Bai, H. Fan, H. Zhang, *et al.*, *J. Mater. Chem. A*, 2015, **3**, 5535.
11 X. H. Liang, X. M. Zhang, W. Liu, D. M. Tang, B. S. Zhang and G. B. Ji, *J. Mater. Chem. C*, 2016, **4**, 6816.
12 H. Yang, M. Cao, Y. Li, H. Shi, Z. Hou, X. Fang, *et al.*, *Adv. Opt. Mater.*, 2014, **2**, 214.
13 M. S. Cao, X. X. Wang, W. Q. Cao and J. Yuan, *J. Mater. Chem. C*, 2015, **3**, 6589.
14 Y. C. Qing, D. D. Min, Y. Y. Zhou, F. Luo and W. C. Zhou, *Carbon*, 2015, **86**, 98.
15 M. Q. Ning, M. M. Lu, J. B. Li, Z. Chen, Y. K. Dou, C. Z. Wang, *et al.*, *Nanoscale*, 2015, **7**, 15734.
16 Y. F. Wang, D. L. Chen, X. Yin, P. Xu, F. Wu and M. He, *ACS Appl. Mater. Interfaces*, 2015, 7, 26226.
17 Y. C. Qing, W. C. Zhou, F. Luo and D. M. Zhu, *Ceram. Int.*, 2016, **42**, 16412.
18 B. Aïssa, A. Ali, K. A. Mahmoud, T. Haddad and M. Nedil, *Appl. Phys. Lett.*, 2016, **109**, 043109.

19 D. C. Wei, Y. Q. Liu, Y. Wang, H. L. Zhang, L. P. Huang and G. Yu, *Nano Lett.*, 2009, **9**, 1752.

20 J. Feng, F. Z. Pu, Z. X. Li, X. H. Li, X. Y. Hu and J. T. Bai, *Carbon*, 2016, **104**, 214.

21 M. K. Han, X. W. Yin, H. Wu, Z. X. Hou, C. Q. Song, X. L. Li, *et al.*, *ACS Appl. Mater. Interfaces*, 2016, **8**, 21011.

22 Q. Zeng, X. Xiong, P. Chen, Q. Yu, Q. Wang, R. Wang and H. Chu, *J. Mater. Chem. C*, 2016, **4**, 10518.

23 L. B. Kong, Z. W. Li, L. Liu, R. Huang, M. Abshinova, Z. H. Yang, *et al.*, *Int. Mater. Rev.*, 2013, **58**, 203.

24 V. M. H. Ng, H. Huang, K. Zhou, P. Lee, W. Que, J. Z. Xu and L. B. Kong, *J. Mater. Chem. A*, 2017, **5**, 3039.

25 Y. C. Qing, W. C. Zhou, F. Luo and D. M. Zhu, *Carbon*, 2010, **4**, 84074.

26 X. L. Zheng, J. Feng, Y. Zong, H. Miao, X. Y. Hu, J. T. Bai and X. H. Li, *J. Mater. Chem. C*, 2015, **3**, 4452.

27 C. Brosseau, *J. Appl. Phys.*, 2002, **91**, 3197.

28 Y. C. Qing, W. C. Zhou, F. Luo and D. M. Zhu, *J. Mater. Chem. C*, 2013, **1**, 536.

29 C. Brosseau, P. Quéffélec and P. Talbot, *J. Appl. Phys.*, 2001, **89**, 4532.

30 X. Li, H. Yi, J. Zhang, J. Feng, F. Li, D. Xue, *et al.*, *J. Nanopart. Res.*, 2013, **15**, 1472.

31 J. Liu, W. Q. Cao, H. B. Jin, J. Yuan, D. Q. Zhang and M. S. Cao, *J. Mater. Chem. C*, 2015, **3**, 4670.

32 B. Adohi, A. Mdarhri, C. Prunier, B. Haidar and C. Brosseau, *J. Appl. Phys.*, 2010, **108**, 074108.

33 H. Lv, Y. Guo, Z. Yang, Y. Cheng, L. P. Wang, B. Zhang, Y. Zhao, Z. J. Xu and G. Ji, *J. Mater. Chem. C*, 2017, **5**, 491.

34 G. Wang, Z. Gao, S. Tang, C. Chen, F. Duan, S. Zhao, S. Lin, Y. Feng, L. Zhou and Y. Qin, *ACS Nano*, 2012, **6**, 11009.

35 B. Adohi, V. Laur, B. Haidar and C. Brosseau, *Appl. Phys. Lett.*, 2014, **104**, 082902.

36 A. Dimiev, W. Lu, K. Zeller, B. Crowgey, L. C. Kempel and J. M. Tour, *ACS Appl. Mater. Interfaces*, 2011, **3**, 4657.

37 J. Shang, Y. Zhang, L. Yu, X. Luan, B. Shen, Z. Zhang, *et al.*, *J. Mater. Chem. A*, 2013, **1**, 884.

38 B. Wen, M. S. Cao, M. M. Lu, W. Q. Cao, H. L. Shi, J. Liu, *et al.*, *Adv. Mater.*, 2014, **26**, 3484.

39 Y. C. Qing, Y. Mu, Y. Y. Zhou, F. Luo, D. M. Zhu and W. C. Zhou, *J. Eur. Ceram. Soc.*, 2014, **34**, 2229.

40 H. L. Lv, G. B. Ji, X. H. Liang, H. Q. Zhang and Y. W. Du, *J. Mater. Chem. C*, 2015, **3**, 5056.

41 Y. C. Qing, X. Wang, Y. Y. Zhou, Z. B. Huang, F. Luo and W. C. Zhou, *Compos. Sci. Technol.*, 2014, **102**, 161.

42 W. L. Song, M. S. Cao, M. M. Lu, S. Bi, C. Y. Wang, J. Liu, *et al.*, *Carbon*, 2014, **66**, 67.

43 W. L. Song, M. S. Cao, M. M. Lu, J. Liu, J. Yuan and L. Z. Fan, *J. Mater. Chem. C*, 2013, **1**, 1846.

44 J. Feng, F. Z. Pu, Z. X. Li, X. H. Li, X. Y. Hu and J. T. Bai, *Carbon*, 2016, **104**, 214.

45 X. H. Li, J. Feng, H. Zhu, C. H. Qu, J. T. Bai and X. L. Zheng, *RSC Adv.*, 2014, **4**, 33619.

46 W. Q. Cao, X. X. Wang, J. Yuan, W. Z. Wang and M. S. Cao, *J. Mater. Chem. C*, 2015, **3**, 10017.

47 Y. C. Qing, J. Wang, H. Y. Wang, F. Luo and W. C. Zhou, *RSC Adv.*, 2016, **6**, 80424.